Reconstruction of the 236 U input function for the N ortheast A tlantic O cean: Implications for 129 I / 236 U and 236 U / 238 U -based tracer ages

Marcus Christl, Núria Casacuberta, Christof Vockenhuber, Christoph Elsässer, Pascal Bailly Du Bois, Jürgen Herrmann, Hans-arno Synal

AGU PUBLICATIONS

JGR

Journal of Geophysical Research: Oceans

RESEARCH ARTICLE

10.1002/2015JC011116

Reconstruction of the ^{236}U input function for the Northeast Atlantic Ocean: Implications for $^{129}I/^{236}U$ and $^{236}U/^{238}U$-based tracer ages

Marcus Christl[1], Núria Casacuberta[1], Christof Vockenhuber[1], Christoph Elsässer[2], Pascal Bailly du Bois[3], Jürgen Herrmann[4], and Hans-Arno Synal[1]

[1]Laboratory of Ion Beam Physics, ETH Zurich, Switzerland, [2]Institut für Umweltphysik, University of Heidelberg, Heidelberg, Germany, [3]IRSN/PRP, Laboratoire de Radioécologie, Cherbourg-Octeville, France, [4]Bundesamt für Seeschifffahrt und Hydrographie, Hamburg, Germany

Abstract A reconstruction of historical discharges of ^{236}U into the Northeast Atlantic Ocean by nuclear installations is presented. The nuclear reprocessing facilities Sellafield (SF), Great Britain (GB) and La Hague (LH), France and potentially also the nuclear fuel processing installation Springfields (SP), GB represent the main contributors of ^{236}U in the Northeast Atlantic Ocean. Because data on ^{236}U releases is lacking, ^{236}U discharges from SP and SF are estimated based on the U-isotopic systematics found in the discharges from LH. The resulting reconstruction of ^{236}U releases indicates that, until 2013, a total of (95 ± 32) kg of ^{236}U was discharged from SF, SP, and LH. In a second step, the reconstructed ^{236}U releases are combined with ^{129}I data from literature and oceanic and atmospheric box models are used to derive the $^{129}I/^{236}U$ and $^{236}U/^{238}U$ input functions that, for example, can be used to calculate tracer ages of Atlantic Waters in the Arctic Ocean. Our conceptual results show that the combination of $^{129}I/^{236}U$ and $^{236}U/^{238}U$ generally allows the estimation of tracer ages over the past approximately 25 years if contributions of ^{236}U from global fallout are considered. Finally, as a proof of concept, the new method is applied to calculate tracer ages of Arctic Ocean surface samples (collected in 2011/2012) and the results are in good agreement with literature data. We conclude that the combination of $^{129}I/^{236}U$ with $^{236}U/^{238}U$ in a dual tracer approach provides a sensitive tool for the calculation of tracer ages and ventilation rates in the North Atlantic region.

Key Points:
- First reconstruction of the oceanic ^{236}U input by nuclear reprocessing
- Presentation of a new $^{129}I/^{236}U$ and $^{236}U/^{238}U$-based dual tracer concept
- Calculation of $^{129}I/^{236}U$ and $^{236}U/^{238}U$-based tracer ages in the Arctic Ocean

Correspondence to:
M. Christl,
mchristl@ethz.ch

Citation:
Christl, M., N. Casacuberta, C. Vockenhuber, C. Elsässer, P. Bailly du Bois, J. Herrmann, and H.-A. Synal (2015), Reconstruction of the ^{236}U input function for the Northeast Atlantic Ocean: Implications for $^{129}I/^{236}U$ and $^{236}U/^{238}U$-based tracer ages, *J. Geophys. Res. Oceans, 120*, 7282–7299, doi:10.1002/2015JC011116.

Received 7 JUL 2015
Accepted 12 OCT 2015
Accepted article online 15 OCT 2015
Published online 9 NOV 2015

1. Introduction

Anthropogenic radionuclides have been (and are) extensively used as transient tracers in oceanography. The oceanic distribution of radionuclides (such as ^{3}H, ^{14}C, ^{90}Sr, ^{137}Cs, etc.) produced during the period of atmospheric nuclear bomb tests provided valuable information about the ventilation of the upper ocean and about the formation of deep water [*Broecker and Peng*, 1982]. Further, the regional and point-like release of a suite of different radionuclide contaminants (such as ^{3}H, ^{90}Sr, ^{99}Tc, ^{125}Sb ^{129}I, ^{137}Cs, and transuranic actinides) by the nuclear reprocessing facilities Sellafield (formerly Windscale), Great Britain (later termed SF) and La Hague, France (later termed LH) into the Northeast Atlantic Ocean (Figure 1) triggered numerous oceanographic tracer studies [*Alfimov et al.*, 2004; *Bailly du Bois et al.*, 1993, 2012; *Herrmann et al.*, 1995; *Karcher et al.*, 2004; *Nies*, 1990]. These studies investigated the local distribution and the dispersion of anthropogenic radionuclides and were able to quantify timescales of regional ocean circulation. In particular, the release of ^{129}I mainly from LH [*Raisbeck et al.*, 1995] was used to trace Atlantic water masses throughout the Arctic Ocean into the deep North Atlantic Ocean [*Alfimov et al.*, 2004; *Smith et al.*, 2005]. Furthermore, the well-known and distinct input function of ^{129}I was used to calculate transit times or so called tracer ages of Atlantic water masses in the Arctic and North Atlantic Ocean [*Alfimov et al.*, 2006; *Smith et al.*, 2005, 2011]. Such concentration-based tracer ages, however, had to be corrected for dilution effects which unavoidably occur while the water masses are being transported. As an alternative and more robust method for the calculation of tracer ages in the Arctic Ocean the ratio of different tracers was suggested, and, for example, the radionuclides ^{137}Cs and/or ^{129}I were successfully combined with ventilation tracers like CFCs to get a comprehensive picture of water mass transit and ventilation times in the Arctic Ocean [*Smith et al.*, 1998, 2005, 2011]. The application of CFCs and ^{129}I in oceanographic studies, however, is

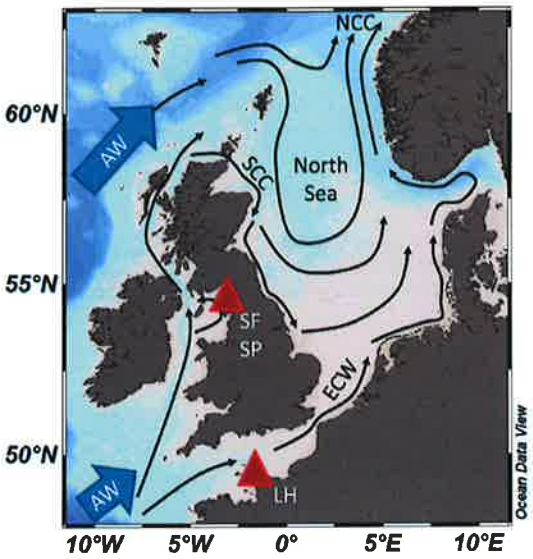

Figure 1. Map of the North Sea region. The locations of the nuclear reprocessing plants Sellafield (SF) and La Hague (LH) as well as the nuclear fuel producing facility Springfields (SP) are marked by red triangles. The black arrows indicate the prevailing surface water circulation pattern and major currents (ECW: English Channel Waters, SCC: Scottish Coastal Current, NCC: Norwegian Coastal Current). The blue arrows indicate the flow direction of Atlantic Waters in that region.

increasingly challenged by the declining shape of the input functions [*Bullister*, 2014; *Michel et al.*, 2012] that do not allow anymore the unequivocal calculation of tracer ages for young water masses (ventilation age shorter than 15–20 years).

To assess the rapid transit times of Atlantic waters in the Arctic Ocean a dual tracer approach has been suggested that combines two radionuclides released from nuclear reprocessing (^{129}I and ^{137}Cs) and uses the ^{129}I/^{137}Cs ratio for the calculation of tracer ages in the Arctic Ocean [*Smith et al.*, 2011]. It has been shown in this study that the dynamic range of the ^{129}I/^{137}Cs method (given by the shape of the input function) yields unique tracer ages for waters labeled between about 1990 and 2005 (end of the published input function). However, dilution effects are not negligible when applying the ^{129}I/^{137}Cs ratio for tracer age estimations because the initial ^{129}I/^{137}Cs ratio is altered as the water mass is transported through the Arctic Ocean by mixing with Atlantic waters carrying the global fallout background of ^{137}Cs and ^{129}I concentrations. Another drawback for the practical application of the ^{129}I/^{137}Cs method in oceanographic studies is that the radiometric determination of ^{137}Cs in sea water currently requires very large (20–30 L) sample volumes [*Smith et al.*, 2011].

Over the past few years anthropogenic ^{236}U ($T_{1/2}$ = 23.5 Myr) has evolved as a new oceanographic tracer [*Casacuberta et al.*, 2014; *Christl et al.*, 2012; *Eigl et al.*, 2011; *Sakaguchi et al.*, 2012; *Winkler et al.*, 2011]. During the period of nuclear bomb tests about 1 t of this radionuclide had been produced [*Sakaguchi et al.*, 2009] and subsequently deposited onto Earth and introduced into the Oceans. The introduction of anthropogenic ^{236}U into the surface oceans raised the ^{236}U/^{238}U ratios (here always reported as atom ratios) from the natural levels (estimated to 10^{-13}–10^{-14}) [*Steier et al.*, 2008] up by several orders of magnitude. For example, in the surface waters of the Atlantic Ocean and the Japanese Sea ^{236}U/^{238}U ratios of (0.5 – 2) × 10^{-9} have been reported [*Casacuberta et al.*, 2014; *Sakaguchi et al.*, 2012]. Furthermore, it has been shown that the anthropogenic ^{236}U signal already has entered the deep Atlantic Ocean [*Christl et al.*, 2012] and that the concentrations of ^{236}U found in different water masses can be well linked to regional hydrography [*Casacuberta et al.*, 2014; *Sakaguchi et al.*, 2012].

Besides the global input of ^{236}U, it is also (locally) released into Northeast Atlantic Ocean with the liquid discharges from the European nuclear fuel reprocessing plants SF and LH (Figure 1). Recently it has been shown that ^{236}U concentrations in the surface waters of the North Sea [*Christl et al.*, 2015] and in the Arctic Ocean (N. Casacuberta et al., unpublished data, 2015) are dominated by ^{236}U from nuclear reprocessing. For example, ^{236}U/^{238}U ratios at the order of 10^{-8} have been measured in North Sea surface waters which are one order of magnitude larger than the ratios found in any other previously reported oceanic surface water sample [*Casacuberta et al.*, 2014; *Eigl et al.*, 2011; *Sakaguchi et al.*, 2012]. The elevated concentrations of ^{236}U could be explained by considering ^{236}U discharges from SF and LH [*Christl et al.*, 2013, 2015].

The fact that ^{236}U discharges from nuclear reprocessing dominate the ^{236}U concentrations in the Northeast Atlantic and Arctic Ocean implies that also ^{236}U can be used to trace Atlantic water masses in the Arctic Ocean. Based on recently published measurements of ^{129}I and ^{236}U in the North Sea it has been suggested to combine ^{236}U with ^{129}I (in a similar way as described above for ^{129}I/^{137}Cs) and to use the combination of two ratios ^{129}I/^{236}U and ^{236}U/^{238}U for the calculation of tracer ages [*Christl et al.*, 2015]. The main advantages

of combining ^{236}U with ^{129}I (and natural occurring ^{238}U) is that these tracers (i) behave conservative in sea water, and (ii) can be analyzed with highest sensitivity in comparably small sample volumes (≈0.5 l for ^{129}I, ≈5 l for ^{236}U) by compact accelerator mass spectrometry (AMS) [*Christl et al.*, 2015; *Vockenhuber et al.*, 2015]. Thus, the combination of $^{129}I/^{236}U$ and $^{236}U/^{238}U$ provides an alternative and sensitive tool for transit time and tracer age estimates of Atlantic Waters in the Arctic Ocean. The knowledge of the $^{129}I/^{236}U$ input function would not only allow the calculation of tracer ages which are, for example, important to constrain circulation changes in the Arctic Ocean [*Karcher et al.*, 2012], it might also provide a suitable tool to determinate the ventilation rates of the deep Arctic Ocean Basins where steep vertical tracer gradients demand for very sensitive tools.

The successful application of the above suggested dual tracer approach, however, crucially depends on two factors. First, the input function of both tracers has to be well known, second, the tracer ratio has to cover a suitable dynamic range that allows the calculation of unequivocal tracer ages (given by the shape of the input function). While the input of ^{129}I into the Northeast Atlantic Ocean mainly from nuclear reprocessing is fairly well known (e.g., summarized in *Michel et al.* [2012]), information about historical ^{236}U discharges is sparse. Previous studies presented some numbers of recent ^{236}U discharges from LH [*Casacuberta et al.*, 2014; *Christl et al.*, 2013] but so far no data on ^{236}U releases are available for SF or any other nuclear installation. Also some data on $^{129}I/^{236}U$ ratios in the releases from LH and SF were reported that indicate a large dynamic range for the new dual tracer approach [*Christl et al.*, 2015]. However, a systematic investigation of the potential of $^{129}I/^{236}U$ and $^{236}U/^{238}U$ as new tools for the calculation of tracer ages including a reconstruction of the historical input of ^{236}U into the Northeast Atlantic Ocean has not been presented yet.

In this paper, a first attempt is made to compile and to reconstruct historical ^{236}U discharges from nuclear installations into the Northeast Atlantic Ocean. The reconstructed ^{236}U discharges are combined with the corresponding ^{129}I data from literature and a simple box model is used to simulate the temporal evolution of the $^{129}I/^{236}U$ and $^{236}U/^{238}U$ ratios in the North Sea (also taking into account the atmospheric input of ^{236}U and ^{129}I from global fallout). Based on the model calibration with ^{129}I, the $^{129}I/^{236}U$ and $^{236}U/^{238}U$ input functions are calculated and the results of the simulations are compared with observations. Finally, the first data set of $^{129}I/^{236}U$ and $^{236}U/^{238}U$ in the Arctic Ocean is used to test and validate the new dual tracer concept.

2. Historical U and ^{236}U Discharges, Data, and Reconstructions

Information about total annual U discharges (by weight mainly consisting of ^{238}U) is accessible for many nuclear installations in Europe but specific information on their ^{236}U content is currently available only for LH (with incomplete temporal coverage). In this section, we try to reconstruct the ^{236}U releases from other nuclear installations in Northwestern Europe based on their documented annual U releases.

2.1. Historical U Discharges From Nuclear Facilities

Over the past two decades (1995–2013) liquid U discharges from nuclear establishments into the Northeast Atlantic Ocean have been documented in the European OSPAR Commission and the British RIFE reports [e.g., *OSPAR*, 2009; *Scottish Environment Protection Agency (SEPA)*, 2010]. According to these annual data, the top three contributors to liquid U discharges to the coastal environment in the time period 1995–2013 are the nuclear fuel production installation Springfields, Lancashire, Great Britain (later termed SP) and the two nuclear reprocessing facilities SF and LH (Figures 1 and 2). We will therefore focus in the following on the reconstruction of total U (and ^{236}U) releases by these three facilities.

The nuclear installations in SF were built in the late 1940s and the nuclear reactors in Windscale (later SF) became operational in 1950/1951. The nuclear facility SP is producing nuclear fuels since the mid-1940s and the operational period of LH started in 1966. Consequently, there is a substantial data gap for all facilities from their commissioning date until 1995.

For LH, additional data on annual U discharges (1966–1994) were made available by AREVA finally covering the full operational time period. Furthermore, additional information on the isotopic composition of the U releases became available for the time period 1966–2012 with only few discontinuities (discussed separately in the next section). We therefore consider the information about total U and ^{236}U discharges from LH as (almost) complete.

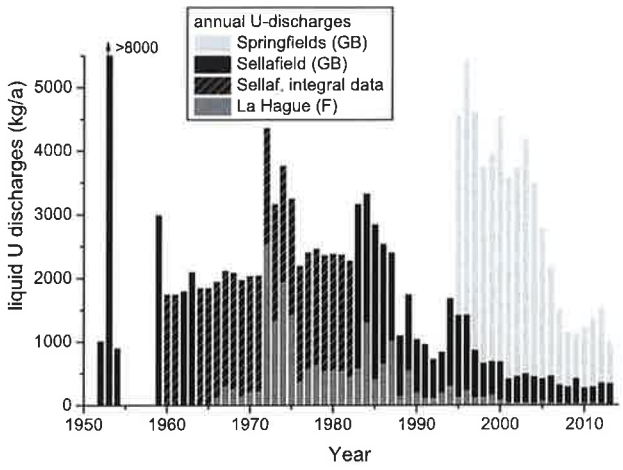

Figure 2. Annual liquid U discharges (stacked columns) from the nuclear reprocessing facilities Sellafield, Great Britain and La Hague, France and the nuclear fuel production installation Springfields, Great Britain as documented (filled bars) in the annual OSPAR and RIFE reports [e.g., *OSPAR*, 2009; *SEPA*, 2010] (additional data were kindly provided by AREVA). The hatched bars indicate calculated annual releases based on integral numbers from literature (see text for details). Before 1995 no data are available for Springfields.

Also for SF, additional data on annual U discharges became available covering the time period 1983–1994. Before this time period almost no data are found about U discharges from SF (ca. 1950–1983). A few numbers on annual releases between 1952 and 1963 (black bars in Figure 2) could be extracted from literature [*Fair and Tweedy*, 1957; *Wix et al.*, 1965] and some integral numbers on U discharges summing up the U releases over several years are available for different time periods [*Hamilton*, 2001; *Hamilton and Stevens*, 1985]. Based on this integral information a constant annual U discharge from SF was assumed for the according years (hatched black bars in Figure 2). No information about the isotopic composition of the U releases or on ^{236}U releases is available for the complete operational period of SF.

For SP no early (before 1995) data on U releases were found in literature although it appears almost certain that U releases occurred over the full operational period. Although representing an important source of U, SP probably did not emit large quantities of ^{236}U since nuclear fuels are dominantly produced from natural U (U_{nat}) that, in this context, contains negligible amounts of ^{236}U (see further discussion in section 2.3.3).

2.2. Documented and Estimated ^{236}U Discharges

The only facility that provided (discontinuous) information about the isotopic composition of liquid U discharges (including ^{236}U) is LH. According to these data (Figure 3a), 22 kg of ^{236}U have been discharged from LH (1966–2012, data gap: 1997–2003). For the other two nuclear facilities considered in this study the ^{236}U discharges have to be estimated. In the following, we first discuss in detail the systematics found in the isotopic composition of U released from LH because this data is key for the following reconstruction of ^{236}U releases from SF. Finally, potential ^{236}U releases from SP are estimated assuming different contributions of ^{236}U from recycled U in the total U discharges.

2.2.1. Isotopic Composition of U Discharges From La Hague

A remarkable time trend is found in the $^{236}U/^{238}U$ ratios of the discharges from LH (black dots in Figure 3b, the green line represents a nonlinear curve fit to the data). The $^{236}U/^{238}U$ ratios evolve from ratios below 10^{-4} in 1965 up to an almost constant value of about 4×10^{-3} for the modern releases, which is in good agreement with reported $^{236}U/^{238}U$ ratios for spent nuclear fuel [*Neghabian et al.*, 1991; *Wolf et al.*, 2005].

The gradual change of $^{236}U/^{238}U$ in the effluents from LH most probably has to do with a change in nuclear technology and related fuel types. In the 1960s and 1970s most of the spent fuel in France and other countries was produced from reactors running on U_{nat} like the *Uranium Naturel Graphite Gaz* reactors (UNGG, France) or the *Magnox* reactors (GB), while nowadays the majority of nuclear reactors in Europe run on U_{enr} (Figure 3c) (data from *Wikipedia* [2015]). In France, the relative contribution of reactors running on U_{enr}

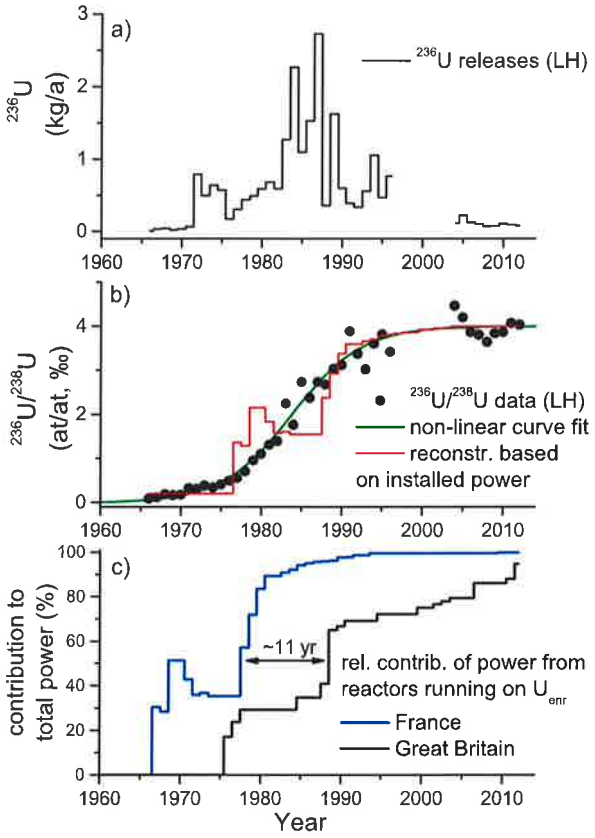

Figure 3. Reported annual ^{236}U discharges from (a) La Hague and (b) corresponding ^{236}U/^{238}U ratios (black dots). The green line in Figure 3b represents a nonlinear curve fit to the reported ^{236}U/^{238}U data using the function $F(x) = A/(1+\exp(-(x-x_0)/dx)$ with the resulting fit parameters: $A = 0.0040 \pm 0.0001$, $x_0 = 1983.8 \pm 0.4$, $dx = 4.3 \pm 0.3$, and reduced $R^2 = 0.98$. The red line in Figure 3b indicates a reconstruction of the ^{236}U/^{238}U ratio in the U discharges from LH based on the relative contribution of reactors running on U_{enr} to the total installed nuclear power in France (blue line in Figure 3c). The black line in Figure 3c indicates the same quantity for Great Britain (data from *Wikipedia* [2015]). Relative to F the curve for GB is shifted by about 11 years.

(mainly pressurized water reactors, PWR) steadily grew in the 1970s and 1980s and today almost all nuclear power in France is produced by such reactors (blue line in Figure 3c).

In the following we will first explain the observed correlation between increased usage of U_{enr} in nuclear reactors and the elevated ^{236}U/^{238}U ratios in the U releases from LH and then use a simple model to reconstruct the reported ^{236}U/^{238}U ratios based on the relative contribution of installed nuclear power running on U_{enr} (the red line Figure 3b already shows the resulting reconstruction).

2.2.2. U Isotopic Systematics in the U Discharges From La Hague

To explain the observed correlation between the use of U_{enr} in nuclear fuels in France and the increased ^{236}U/^{238}U ratios in releases from LH, a simple physical model is used. When considering the three main nuclear reactions of thermal neutrons with ^{235}U and ^{238}U that consume either ^{235}U (^{235}U(n,γ)^{236}U, with a cross section $\sigma_{5,n} = 99$ barn and fission of ^{235}U, $\sigma_{5,f} = 583$ barn) or ^{238}U (^{238}U(n,γ), $\sigma_{8,n} \simeq 2$ barn), the temporal evolution of the U-isotopic composition $R_{5,8}(t) = {}^{235}\mathrm{U}/{}^{238}\mathrm{U}(t)$ and $R_{6,8}(t) = {}^{236}\mathrm{U}/{}^{238}\mathrm{U}(t)$ can be described as:

$$R_{5,8}(t) = R_{5,8\ initial} \cdot e^{-\Phi\left(\sigma_{5,tot}-\sigma_{8,n}\right)t} \quad (1)$$

$$R_{6,8}(t) = R_{5,8\ initial} \cdot f_{5,n} \cdot \left(1-e^{-\Phi\sigma_{5,tot}t}\right) \cdot e^{\Phi\sigma_{8,n}t} \quad (2)$$

where $\sigma_{5,tot} = \sigma_{5,n} + \sigma_{5,f}$, Φ is the neutron flux, and $f_{5,n} = {}^{\sigma_{5,n}}/_{\sigma_{5,tot}}$ reflects the branching fraction for ^{236}U production from ^{235}U. Because $\sigma_{8,n}$ is much smaller than the other two cross sections involved, the relation

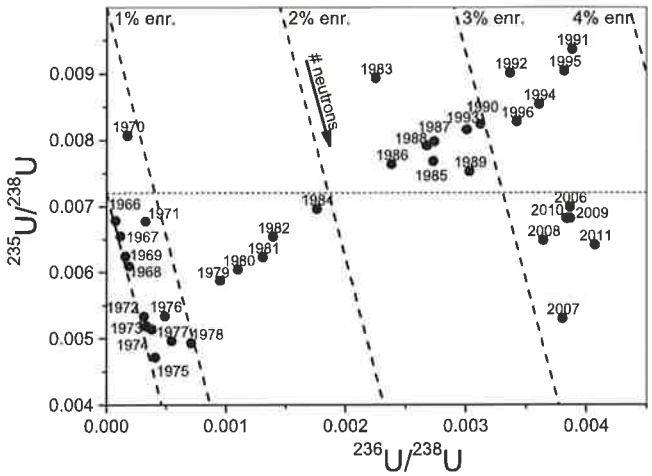

Figure 4. U isotopic systematics in the U discharges from LH. The dots represent the average $^{236}U/^{238}U$ and $^{235}U/^{238}U$ ratio of U releases for each respective year (labels). The dashed lines show the calculated (using equations (1)–(3)) evolution of the U isotopes in a nuclear reactor with increasing irradiation time (number of neutrons) using different degrees of initial enrichment of ^{235}U as a parameter. The horizontal dashed line marks the $^{235}U/^{238}U$ ratio of natural U.

between $R_{5,8}(t)$ and $R_{6,8}(t)$ evolves with time (or number of neutrons, $\Phi \times t$) on a straight line in a $R_{5,8}$ versus $R_{6,8}$ diagram (Figure 4) only depending on the initial degree of enrichment $R_{5,8\ initial}$ (dashed lines in Figure 4).

$$R_{5,8}(t) \cong R_{5,8\ initial} - \frac{R_{6,8}(t)}{f_{5,n}} = R_{5,8\ initial} - 6.89 \cdot R_{6,8}(t) \tag{3}$$

Resolving equation (3) for $R_{6,8} \cong \frac{R_{5,8\ initial} - R_{5,8}(t)}{6.89}$ it becomes clear that nuclear power reactors can only produce high $^{236}U/^{238}U$ ratios (e.g. $>1 \times 10^{-3}$) if they are running on enriched fuel. Nuclear power reactors running on U_{nat} cannot produce high $^{236}U/^{238}U$ ratios because ^{235}U is consumed about seven times more rapidly by fission than by neutron capture. Before high $^{236}U/^{238}U$ ratios can build up in such reactors the fuel is spent and has to be replaced.

Comparing the physical model with the available isotopic data from LH (Figure 4) it becomes evident that the observed trend in the $^{236}U/^{238}U$ ratio of the U the discharges reflects (with a time delay that might depend on many parameters) a transition in nuclear technology: the progressive installation of reactor types (like PWRs) that run on U_{enr} fuel. Since nowadays the majority of reactors in Europe are running U_{enr} the above finding implies that (i) this trend is probably not only present in France and (ii) that future U discharges from nuclear reprocessing will probably carry high $^{236}U/^{238}U$ ratios of about 4×10^{-3}.

2.3. Model-Based Reconstructions of $^{236}U/^{238}U$ Ratios in the U-Releases

2.3.1. Reconstruction of $^{236}U/^{238}U$ Released From La Hague

Based on the above findings, we now try to reconstruct the published $^{236}U/^{238}U$ ratios in the U discharges from LH based (dots in Figure 3b) based on the relative contribution of nuclear power coming from reactors running on U_{enr} (blue line in Figure 3c). We assume that discharges from reactors running on U_{enr} with a delay in time produce discharges with a constant $^{236}U/^{238}U$ ratio of 4×10^{-3} while the others (running on U_{nat}) lead to much lower but also constant $^{236}U/^{238}U$ ratios of 2×10^{-4} in the discharges (compare Figure 4). The partitioning, and thus the mixing between the two above defined end members, in the model, is given by the relative contribution of nuclear power from U_{enr}-based reactors in each corresponding year (blue curve in Figure 3c). The only free parameter in this model is the delay time ($t_{d,power}$) that, in the model, accounts for several unknown parameters like the average time elapsed between usage, storage, and final waste disposal in the fuel cycle. The reported $^{236}U/^{238}U$ ratios from LH are used to calibrate the model by variation of $t_{d,power}$. The best fit of the modeled discharge ratios to the LH data is found for a delay time $t_{d,power} = 10$ years (red line in Figure 3b). With the above calibration, the model is applied in the next section to reconstruct the $^{236}U/^{238}U$ ratio in the U discharges from SF.

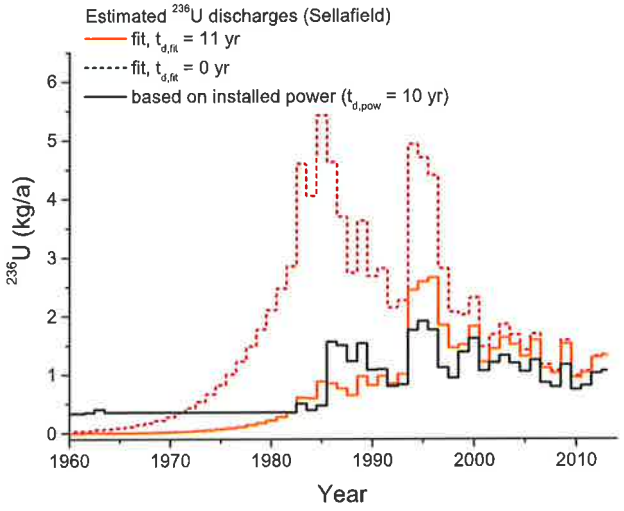

Figure 5. Model-based reconstructions of annual ^{236}U discharges from Sellafield. Different temporal evolutions of the $^{236}U/^{238}U$ ratios in the U discharges from Sellafield are assumed. The red dashed and the orange line are based on the nonlinear fit function from Figure 2b with different delay times to describe the evolution of $^{236}U/^{238}U$. The black line shows a reconstruction based on the relative contribution of power from reactors running on U_{enr} (black curve in Figure 2c) and uses a delay time $t_{d,pow} = 10$ years (see text for details).

2.3.2. Estimated ^{236}U Discharges From Sellafield

No specific information is available about ^{236}U discharges from SF. Based on the above observed systematics in the isotopic signatures of U discharges from LH we suggest reconstructing the ^{236}U releases from SF based on the total U discharges. Therefore the temporal evolution of the $^{236}U/^{238}U$ ratio in the U releases from SF needs to be reconstructed. Our conceptual approach to estimate the $^{236}U/^{238}U$ ratio in the liquid U discharges from SF is based on the assumptions that (i) only reactors running on enriched U produce high $^{236}U/^{238}U$ ratios, and (ii) that the $^{236}U/^{238}U$ ratio in the liquid discharges is correlated (with a delay in time) with the development of advanced nuclear reactors running on U_{enr} (e.g. Advanced Gas cooled Reactors, AGR in GB).

We are aware of the fact that the real situation is more complex, e.g., that LH and SF are handling different kinds of spent fuel from different countries (e.g. Germany, Switzerland, Japan, etc.) and with different irradiation and storage histories. However, also in these countries the majority of installed nuclear power nowadays is based on PWR or boiling water reactors (BWR) that run on U_{enr} (data from *Wikipedia* [2015]). We therefore believe that the increasing trend in the $^{236}U/^{238}U$ ratio in U discharges from LH is also present at SF. This argument is reinforced by comparing the evolution of the relative contribution of reactors running on U_{enr} in GB and F (Figure 3c). Both curves show very similar trends although the development in GB is shifted by about 11 years relative to F due to the strong contribution of MAGNOX reactors (U_{nat}) to total nuclear power production and the later installation of AGRs in GB.

Two different approaches (resulting in three different reconstructions) are chosen to estimate the temporal evolution of the $^{236}U/^{238}U$ ratios in the U discharges and thus the amount of ^{236}U released from SF. In the first and most simple approach, the nonlinear fit function (green line in Figure 3b) that describes the observed time trend of the $^{236}U/^{238}U$ ratios in the discharges from LH is applied with a time delay of $t_{d,fit} = 11$ years (taken from Figure 3c) to calculate the annual release of ^{236}U from SF (orange curve in Figure 5). This scenario describes a situation where the national development of nuclear technology in GB is the dominant factor controlling the isotopic composition in the subsequent U releases. Using the same fit function, a second reconstruction is made without applying any time delay. This scenario rather describes a situation where the national evolution of nuclear power in GB (in particular the high relative contribution of *Magnox* reactors) is not the dominating factor because spent nuclear fuel from many other countries is also processed (e.g. DE, JP; CH, BE, NL) that do not have reactors running on U_{nat}. In that sense, the $t_{d,fit} = 0$ year scenario (red dotted curve in Figure 5) represents a maximum estimate for the annual ^{236}U releases from SF.

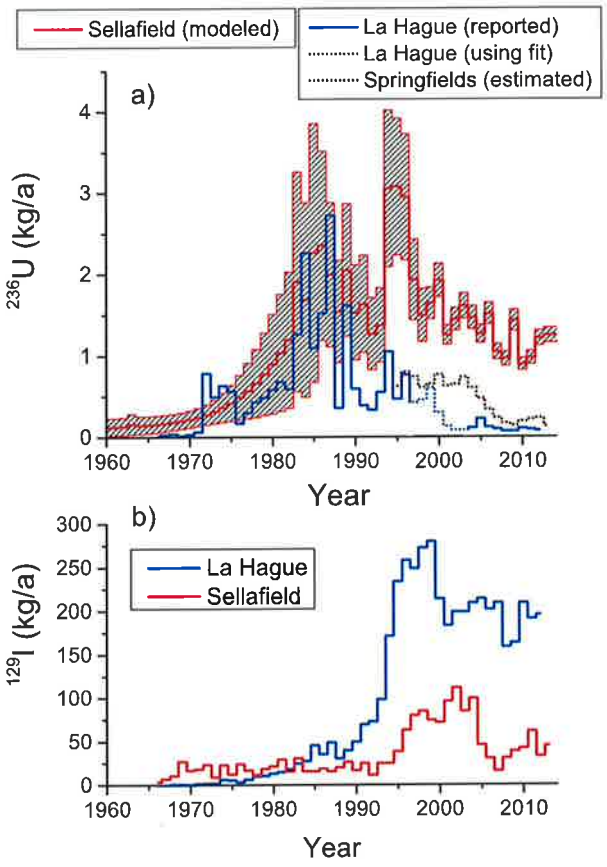

Figure 6. Reconstructed or documented annual discharges of (a) ^{236}U and (b) ^{129}I. The red line in a) represents the average of three different reconstructions of ^{236}U discharges from Sellafield, with the hatched region indicating the resulting uncertainty (error of the mean). The red line in Figure 6b indicates the reported ^{129}I releases from SF [*Michel et al.*, 2012]. The blue curve in Figures 6a and 6b indicates reported ^{236}U and ^{129}I data from La Hague, respectively. The blue dotted line in Figure 6a marks ^{236}U releases that have been calculated based on the reported U discharges from La Hague using the nonlinear fit function from Figure 3b. The brown dotted line in Figure 6a marks the estimated ^{236}U discharges from Springfields (see text for details).

In a second and completely independent approach we use the relative contribution of reactors running on U_{enr} (black curve in Figure 3c) to calculate a third reconstruction of the $^{236}U/^{238}U$ ratios in the U discharges from SF. With the above presented calibration for LH ($t_{d,power}$ = 10 years), the model is applied to calculate the annual releases of ^{236}U from SF (black curve in Figure 5) using the U discharges from SF (Figure 2) as input values.

The three above presented reconstructions of annual ^{236}U discharges from SF (Figure 5) differ significantly before 1990 where the influence of the temporal evolution of the $^{236}U/^{238}U$ ratio in the releases is dominant. After 1990, a reasonable agreement between the different reconstructions is observed because the assumed $^{236}U/^{238}U$ ratios in the discharges are high and less variable. Post 2000, the standard deviation between the different reconstructions is less than 20% implying that the different underlying model assumptions do not have a large effect on the model results. In order to derive one ^{236}U input function for SF the three reconstructions are averaged and the standard error of the mean is used as an estimate for the uncertainty (red curve and shaded region in Figure 6a). In this averaged scenario the total amount of ^{236}U discharged from SF is (62 ± 31) kg, which is 2–3 times more than the total amount of 23.5 kg ^{236}U discharged from LH (blue curve in Figure 6a and see also Table 1).

2.3.3. Estimated ^{236}U Discharges From Springfields

It is not clear if significant amounts of ^{236}U have been discharged from this facility since the majority of U_{enr} is produced from U_{nat} during nuclear fuel production performed by this plant. Consequently, the large

Table 1. ^{236}U Discharges Into the Northeast Atlantic Ocean[a]

Facility (Time Period)	$^{236}U/^{238}U$ Reconstruction	^{236}U Released (kg)	Average/ Total (kg)
Sellafield (1952–2013)	fit LH data (t_d = 11 years)	42.1	62 ± 31
	fit LH data (t_d = 0 year)	97.5[b]	
	nuclear reactor types	47.4	
La Hague (1966–2012)	documented data		23.5
	gaps: calculated from fit		
Springfields (1995–2013)	estimated (2‰)		9 ± 9
		Total	95 ± 32

[a]Total estimated or documented ^{236}U discharges into the Northeast Atlantic Ocean from the nuclear reprocessing facilities Sellafield (GB) and La Hague (F) and from the nuclear fuel production installation Springfields (GB) for the given time periods. The second column indicates the underlying model/data source for the reconstruction of the $^{236}U/^{238}U$ ratios over time.
[b]This value was used for SF in previous studies [*Casacuberta et al.*, 2014; *Christl et al.*, 2013].

amounts of U that have been discharged from SP since 1995 (Figure 2) most probably consisted of U_{dep} from the enrichment of U_{nat} with negligible amounts of ^{236}U. Nevertheless, ^{236}U might be present in the discharges if the produced nuclear fuel is blended with U_{enr} from the enrichment of U that was recycled from spent fuel. In this case, the U discharges would consist of a mixture of both U_{dep} from the enrichment of U recycled from spent fuel and U_{dep} from the enrichment of uranium from U_{nat}. To get at least a rough estimate of the possible amount of ^{236}U discharged from SP we assume that the produced fuel is blended with 10% U_{enr} that was recycled from spent fuel with a ^{236}U content of approximately 2×10^{-3} in the resulting discharges of U_{dep} (the data of the isotopic composition of different compounds were taken from *WISE* [2014], after *Neghabian et al.* [1991]). Based on this estimation (orange dotted line in Figure 6a) about 9 kg of ^{236}U have potentially been discharged from SP. The uncertainty of the above estimation was calculated by varying the relative contribution of U_{enr} recycled from spent fuel between 0% and 20%, resulting in a possible range of total ^{236}U discharges from SP between 0 kg and 18 kg (Table 1).

2.4. Discussion of the Combined ^{236}U Discharges

Combining all the above assumptions and reconstructions, the total estimated amount of ^{236}U released by the two reprocessing plants SF and LH and from the nuclear fuel production installation SP sums up to (95 ± 32) kg (Table 1). Although this number agrees within uncertainties with previous estimates (about 120 kg) [*Casacuberta et al.*, 2014] it is comparably low. This is explained by the fact that previous estimations did not take into account the possible time delay in the $^{236}U/^{238}U$ trend from SF and therefore were based on the $t_{d,fit} = 0$ year scenario (red dotted line in Figure 5) that, in this study, rather represents a maximum estimate for ^{236}U discharges from SF.

The estimated total amount of ^{236}U discharged into the Northeast Atlantic Ocean also has some implications for the presence of additional sources of ^{236}U in the North Atlantic and Arctic Ocean. Recent studies estimated an inventory from nonfallout sources of about 250 kg and 30 kg in the North West Atlantic and Arctic Ocean, respectively. Based on our results, less than half of these extra 280 kg could have been provided by the nuclear facilities SF, SP, and LH. This implies that either ^{236}U had been discharged into the North Atlantic region by other nuclear installations, or that the total amount of ^{236}U originating from global fallout was significantly larger than 1000 kg (ca. 1500–2000 kg). More ^{236}U data are needed to identify and further constrain the additional sources of ^{236}U.

3. Modeling the Input Function of $^{236}U/^{238}U$ and $^{129}I/^{236}U$

A main goal of this study is to estimate the temporal evolution of the $^{236}U/^{238}U$ and $^{129}I/^{236}U$ ratios in the water masses that are advected from the North Sea via the Norwegian Coastal Current (NCC) into the Arctic Ocean. The nuclear facilities SF, SP, and LH have been identified above as the major sources of ^{236}U (and ^{129}I) in the Northeast Atlantic region. Using the above presented reconstructions of annual ^{236}U discharges (Figure 6a) and the well documented releases of ^{129}I from LH and SF (Figure 6b) the $^{236}U/^{238}U$ and $^{129}I/^{236}U$ input functions can be modeled. The box model calculations presented in the following combine the estimated oceanic inputs of ^{236}U and also account for the atmospheric input of ^{236}U (and ^{129}I) from global fallout.

The role of ^{129}I in the box model is twofold. First we take advantage of the fact that the input function of ^{129}I is well described (Figure 6b) and thus use it to calibrate the model for the simulation of ^{236}U. Second, the modeled ^{236}U is combined with ^{129}I from the model calibration (and with seawater concentrations of ^{238}U

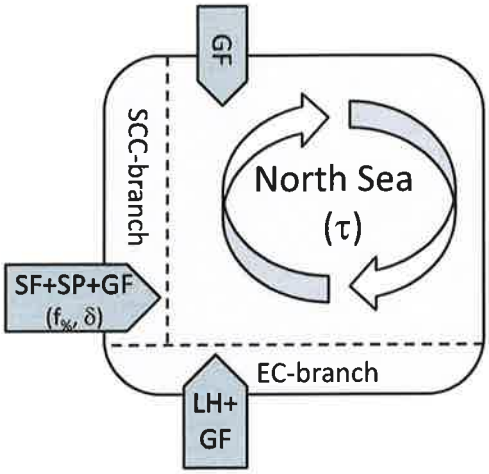

Figure 7. Box model used to simulate the concentrations of ^{236}U and ^{129}I in the North Sea and to calculate the input functions of $^{236}U/^{238}U$ and $^{129}I/^{236}U$. The central box (with water mass exchange rate τ) receives three different tracer inputs: Global fallout (GF), discharges from SF and SP (plus GF) via the Scottish Coastal Current (SCC-branch) and discharges from LH (plus GF) via the English Channel (EC-branch). Additionally, a time delay (δ) and a relative loss rate ($f_{‰}$) can be assigned to the combined SF+SP+GF signal before entering the SCC-branch and the North Sea box.

that are assumed to be constant (3.3 μg/kg) in the model) to derive the temporal evolution of the $^{236}U/^{238}U$ and $^{129}I/^{236}U$ ratios in the North Sea box.

3.1. Box Model Description

A simple one box model is used to calculate the temporal evolution of ^{236}U and ^{129}I concentrations in the North Sea. The model receives three input streams that eventually define the mean residence time of the North Sea waters in the box (Figure 7). The atmospheric input of ^{236}U and ^{129}I from global fallout is calculated separately using an atmospheric multibox model that is coupled to a diffusive global ocean surface model. The output of the global ocean surface model for the North Sea region represents the background level of ^{236}U and ^{129}I without any discharges from nuclear installations. This background signal is present in all three input streams of the box model. In the following, first the atmospheric model and the resulting simulation of the oceanic mixed layer concentrations are presented, then the oceanic inputs (liquid releases from SF, SP and LH) into the North Sea box model are described.

3.1.1. Modeling the Atmospheric Input

The atmospheric input of ^{236}U into the surface ocean is calculated with the two dimensional (laterally averaged) atmospheric multibox model GRACE [*Levin et al.*, 2010]. To simulate the depositional flux of ^{236}U from the atmosphere the most recent version of GRACE that includes the simulation of aerosol-borne radionuclides is used [*Elsässer et al.*, 2015]. The model was calibrated with measured data of ^{137}Cs, ^{90}Sr, ^{210}Pb, SF_6, ^{14}C, and ^{7}Be, and therefore seems appropriate for the simulation of the depositional flux of bomb produced and aerosol-borne ^{236}U. The model represents the main features of the global atmosphere: a vertical division into planetary boundary layer, free troposphere and three stratospheric subdivisions. The horizontal breakdown of the model is 30° in the free troposphere and stratospheric layers which represents the three main atmospheric circulation cells (Hadley, Ferrel and Polar cell). The resolution of the boundary layer is enlarged to 10° per box [*Elsässer et al.*, 2015]. Since major atmospheric processes show variations on the latitudinal scale, the 2-D setup is a reasonable first-order approach for the simulation of ^{236}U deposition. For the implementation of ^{236}U it was assumed that a total of 900 kg of ^{236}U [*Sakaguchi et al.*, 2009] was released into the atmosphere at varying altitudes. The temporal and spatial distribution of the atmospheric ^{236}U source follows the listing of atmospheric nuclear weapon tests as given in the UNSCEAR 2000 report [*UNSCEAR*, 2000]. Following earlier approaches, we assume that only thermonuclear weapons (with a fusion stage) contribute to the production of globally dispersed ^{236}U [*Winkler et al.*, 2011]. The fission yield (MT TNT equivalent) of these devices is used as a proxy for both ^{236}U production and its altitudinal distribution in the atmosphere [*Peterson*, 1970].

The output of the GRACE model, the depositional flux of ^{236}U in 10° latitude bins (the depositional flux at 50°–60°N, is shown as an example by the red curve in Figure 8), is fed into a diffusive global surface ocean model with 1° × 1° lateral resolution and a mixed layer thickness of 50 m to calculate the temporal evolution of the fallout derived ^{236}U concentration in the mixed layer. The input into each box is given by: $dm_{p,i}/dt = p_i \times A_{surf,i}$ where i denoptes the number and $A_{surf,i}$ the surface area of each box, while p_i is the atmospheric input (at/cm^2/s) taken from GRACE. The horizontal exchange is calculated according to: $dm_{h,i}/dt = -Kd_h \times dc_i/dq_{i,xy} \times A_{i,xy}$ where Kd_h represents the horizontal eddy diffusion coefficient (cm^2/s), c_i is the ^{236}U concentration in each box (at/cm^3), q_i denotes the horizontal distance (x or y) to each neighboring box, and $A_{i,xy}$ represents the cross sectional area of box i in x or y direction (note that the according areas and distances are calculated under the assumption that the boxes are located on the surface of an ideal

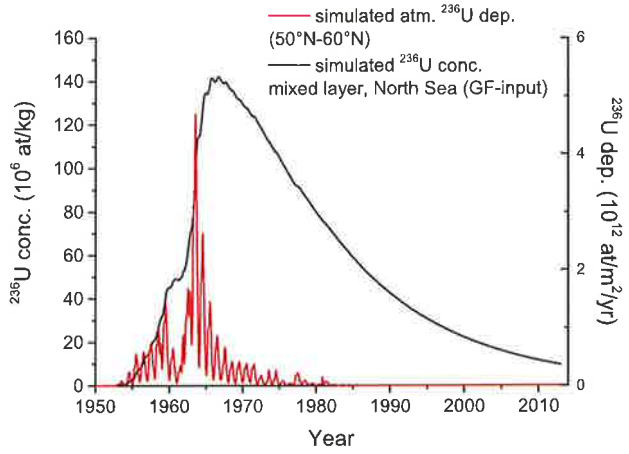

Figure 8. Simulated atmospheric deposition of ^{236}U using the two dimensional atmospheric box model GRACE [*Elsässer et al.*, 2015; *Levin et al.*, 2010]. As an example, the depositional flux of ^{236}U in the latitudinal band 50°N-60°N is shown (red curve). The GRACE model output is fed into a diffusive global ocean surface model (lateral resolution of 1°×1°, mixed layer depth: 50 m). Model grid point 55°N, 5°E is selected as a representative for the temporal evolution of the ^{236}U surface concentration in the North Sea (black line).

sphere). The vertical exchange (loss of ^{236}U) is calculated according to: $dm_{v,i}/dt = -Kd_v \times dc_i/ML \times A_{surf,i}$ with Kd_v: vertical eddy diffusion coefficient (cm^2/s) and ML: mixed layer depth. The simple model does not contain an advective term, and other oceanic processes like water mass up/downwelling are neglected. The intention for this rather simple model setup is to get a rough estimate of the GF background in the North Sea region (surface layer) without any inputs from nuclear reprocessing rather than looking at regional (latitudinal) differences of the atmospheric input pattern or at details of the oceanic distribution of this nuclide.

The turbulent horizontal and vertical diffusion coefficients were tuned so that the modeled ^{236}U concentrations in the North Atlantic Ocean agree with the measured surface concentrations in the Northwest Atlantic Ocean in the year 2010 [*Casacuberta et al.*, 2014]. The resulting diffusion coefficients ($Kd_v = 0.05$ cm^2/s, $Kd_h = 5 \times 10^6$ cm^2/s) agree well with literature values [e.g., *Wright and Stocker*, 1992]. The above model calibration implies that the surface concentrations in the Northwestern Atlantic Ocean are not significantly affected by ^{236}U from nuclear reprocessing.

Finally, the temporal evolution of the ^{236}U concentration at model grid point 55°N, 5°E is arbitrarily chosen as reference curve ($c_{GF}(t)$, black curve in Figure 8) for the background concentration in the North Sea box without any discharges from nuclear installations. The box model results do not depend on the detailed location of the reference point in the North Sea region.

The atmospheric deposition of ^{129}I from global fallout is not explicitly simulated. Instead, the contribution ^{129}I from global fallout is calculated from the GF input of ^{236}U assuming a fixed ^{129}I/^{236}U atom ratio of 0.1 (corresponding to a total of 50 kg ^{129}I produced during nuclear weapons tests [*Hou et al.*, 2009]). The resulting ^{129}I background level in the North Sea region (GF-input, Figure 9) corresponds well with the reported oceanic ^{129}I level from nuclear weapons tests (dashed horizontal line in Figure 9, after *He et al.* [2013]).

3.1.2. Modeling the Liquid Releases

Following earlier modeling studies using ^{129}I [*Orre et al.*, 2010; *Smith et al.*, 2005] it is assumed that the oceanic discharges from LH, SF, and SP enter the North Sea box where they are first mixed and then advected via the NCC into the Arctic Ocean. In the model, the box is fed by three input streams representing (i) Atlantic Waters that enter the North Sea only carrying the global fallout signal ($c_{AW}(t) = c_{GF}(t)$, from the above ocean surface model), (ii) the Scottish Coastal Current (SCC-branch) carrying the tracer signal from GF, SP and SF:

$$c_{SCC}(t) = P_{SF+SP}(t-\delta) \times f_{\%}/F_{SF} + c_{AW}(t) \quad (4)$$

with F_{SF}: annual water mass flux passing by SF (m^3/yr), P_{SF+SP}: annual release of ^{236}U or ^{129}I from SP and SF (at/yr), $f_{\%}$: fraction of P_{SF+SP} that enters the NS box, and δ: delay time (years) for P_{SF+SP} arriving at the Nord Sea box), and (iii) English Channel Waters (EC-branch) carrying the tracer signal from GF and LH:

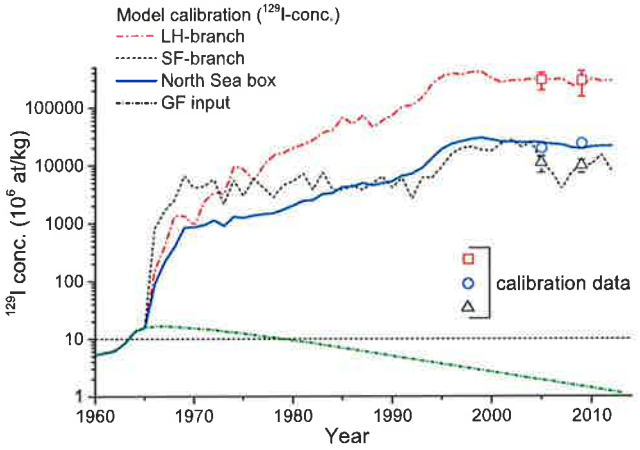

Figure 9. Box model calibration with ^{129}I: The black dashed and the red dash-dotted lines represent the modeled ^{129}I concentrations in the SF-branch and LH-branch, respectively. The green short dash-dotted line displays the ^{129}I modeled concentration in the North Sea due to global fallout (GF). The blue circles represent the geometric mean of the whole data set for each year, while the red squares and the black triangles indicate the arithmetic mean for each branch (SF and LH) and respective year.

$$c_{EC}(t) = P_{LH}(t)/F_{EC} + c_{AW}(t) \tag{5}$$

with P_{LH}: annual release of ^{236}U or ^{129}I from LH (at/yr), F_{EC}: annual water mass flux through the English Channel). Finally, the tracer concentrations in the North Sea box are calculated in 1 year time steps:

$$c_{NS}(t+\Delta t) = c_{NS}(t) + (F_{EC}\times c_{EC}(t+\Delta t) + F_{SCC}\times c_{SCC}(t+\Delta t) + F_{AW}\times c_{AW}(t+\Delta t) - (F_{EC}+F_{SCC}+F_{AW})\times c_{NS}(t))\times \frac{\Delta t}{V_{NS}} \tag{6}$$

Inserting equations (4) and (5) and replacing $(F_{EC}+F_{SCC}+F_{AW})/V_{NS}$ (volume of the North Sea $V_{NS} \approx$ 100'000 km^3) by the water mass exchange rate τ (1/yr), equation (6) can be written as:

$$c_{NS}(t+\Delta t) = c_{NS}(t) + \left(\frac{P_{LH}(t+\Delta t)}{V_{NS}} + \frac{P_{SF+SP}(t-\delta+\Delta t)\times f_{\%}}{V_{NS}} + \tau\times c_{AW}(t+\Delta t) - \tau\times c_{NS}(t)\right)\times \Delta t \tag{7}$$

^{129}I is used to calibrate the model. First, the model is fitted to the measured ^{129}I concentrations in the SCC- and EC-branch waters by varying $f_{\%}$, F_{SF}, and F_{EC}. Then, the ^{129}I concentrations in the North Sea box are fitted by adjusting F_{AW} (discussed below).

Note that the individual values of the fluxes F_{EC}, F_{SCC}, and F_{AW} do not have an influence on the modeled tracer concentration in the North Sea box which is a function of $f_{\%}$, δ, and τ only (equation (7)).

3.2. Box Model Calibration and Results

Combining all above derived tracer inputs (SF plus SP, LH, and GF) the box model is applied to simulate the concentrations of ^{236}U and ^{129}I in the North Sea and to calculate ^{236}U/^{238}U and ^{129}I/^{236}U ratios that finally represent the tracer input functions for the Arctic Ocean.

3.2.1. Calibration With ^{129}I

As stated above, ^{129}I is used to calibrate the box model and published ^{129}I discharges from LH and SF (Figure 6b) [*Michel et al.*, 2012] are used as input values. For the model calibration two large ^{129}I data sets from 2005 and 2009 covering the whole North Sea area are available [*Christl et al.*, 2015; *Michel et al.*, 2012]. According to the geographic location a subset of ^{129}I samples is selected from each data set as representative for the SCC (carrying the SF plus SP signal, black triangles in Figure 9) and for the EC-branch (carrying the LH signal, red squares in Figure 9), respectively (for the selection of data points see *Christl et al.* [2015, Table 1]). Following earlier studies [*Michel et al.*, 2012], the geometric mean of each full data set is calculated and interpreted as a representative of the average ^{129}I concentration in the North Sea for each respective year (open circles in Figure 9). The best fit between modeled branches (dashed/dotted lines in Figure 9) and data (open symbols in Figure 9) is found for F_{EC} and F_{SCC} values of 0.1 Sv and 0.3 Sv (1 Sv = 10^6 m^3/s), respectively. For the North

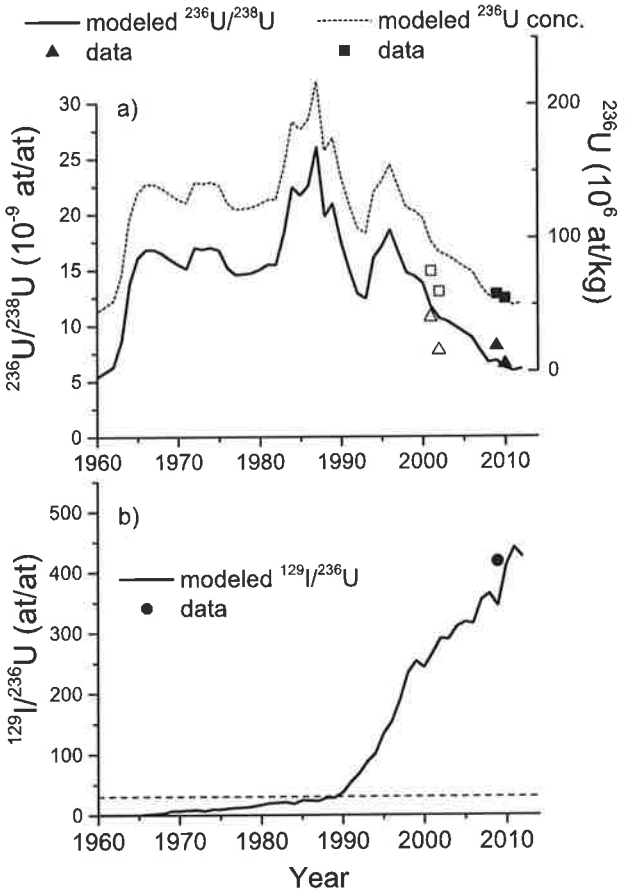

Figure 10. Modeled versus. measured ^{236}U data: the bold lines represent the (a) modeled evolution of the $^{236}U/^{238}U$ and (b) $^{129}I/^{236}U$ ratios over time (left y axes). The dashed line in Figure 10a shows the modeled ^{236}U concentration (right y axis, shifted up for better visibility). Filled data points indicate the geometric means of all ^{236}U concentrations and $^{236}U/^{238}U$ ratios measured in the North Sea in 2009 and 2010 and the geometric mean of all measured $^{129}I/^{236}U$ ratios in 2009. The open symbols are based on two data points each and therefore are not considered representative for the whole North Sea (indicative values). The dashed horizontal line marks the level from which on (up) the $^{129}I/^{236}U$ ratio potentially can be used for the calculation of tracer ages.

Sea box model calibration a total water mass residence time $1/\tau=2.2$ *yr*, a delay $\delta=0$ *yr* (no delay), and a loss rate $f_{\%}=50\%$ is found. These values are in reasonable agreement with data from other studies that report a mean water residence time of 1–2 years for the North Sea [*De Wilde et al.*, 1992] and a transit time of 0.2–2 years for waters originating from SF entering the North Sea [*Povinec et al.*, 2003].

3.2.2. Model Results, Comparison With Measured Data

With the above model calibration the temporal evolution of the ^{236}U concentration and the resulting $^{236}U/^{238}U$ and $^{129}I/^{236}U$ ratios in the North Sea box are calculated (lines in Figures 10a and 10b). The simulations are compared with the available data of ^{236}U, $^{236}U/^{238}U$, and $^{129}I/^{236}U$ in the North Sea (symbols in Figure 10). To compare the model results with measurements, two comprehensive data sets of ^{236}U in the North Sea are available for the years 2009 [*Christl et al.*, 2013, 2015] and 2010 (N. Casacuberta et al., unpublished data, 2015). Again, the geometric mean of each data set was calculated as a representative for the average concentration or ratio in the corresponding year (filled symbols in Figure 10). Additionally, two data points for ^{236}U (and $^{236}U/^{238}U$) are available for the years 2001 and 2002, respectively [*Christl et al.*, 2013]. These single values are not considered representative for the whole North Sea and displayed as indicative values only (open symbols in Figure 10a). Only for the year 2009 $^{129}I/^{236}U$ ratios are available for comparison. The geometric mean of the measured $^{129}I/^{236}U$ ratios is in reasonable agreement with the simulation (Figure 10b).

3.3. Discussion of the Model Results

Generally, a good agreement of the modeled ^{236}U data (ratios and concentrations) with the measurements is found (Figure 10). We note that the model was not tuned to fit the ^{236}U data since only ^{129}I was used for calibration. This implies that the underlying estimations of ^{236}U releases from nuclear facilities into the North East Atlantic Ocean are reasonable (at least for the past about 15 years). At the current stage, however, the uncertainties of the calculated $^{236}U/^{238}U$ and $^{129}I/^{236}U$ input functions are large and cannot be precisely estimated for two main reasons. First, the model calibration is not sensitive to early releases (e.g., before 2000) since the water mass residence time in the North Sea is low (about 2 years in the model) and calibration data are available only for more recent years. Second, the uncertainty in the liquid discharges of ^{236}U is very large for the early releases (mainly due to the unknown history of ^{236}U discharges from SF), while it is at the order of 20% for the past about 20 years. The (systematic) uncertainties in the ^{236}U discharges are still very large and more (historical) ^{236}U data or reconstructions, e.g., from annually growing marine species are needed to improve the knowledge on ^{236}U discharges into the Northeast Atlantic Ocean and therefor the quality of the modeled input functions.

3.4. Implications for the Calculation of Transit Times

According to the above presented dual tracer concept the $^{236}U/^{238}U$ and $^{129}I/^{236}U$ ratios of a water mass (sampled e.g., in the Arctic Ocean), that had been labeled in the North Sea with a distinct tracer signal, can be used to determine its tracer age or the transit time of the water mass from the North Sea to the sampling location. In the following, the simulated $^{236}U/^{238}U$ and $^{129}I/^{236}U$ input functions (bold black curves in Figure 10a and 10b) are used as a best estimate for the temporal evolution of the tracer signal and some implications for the estimation of tracer ages of Atlantic Waters in the Arctic Ocean are discussed (in this context transit time and tracer age are used synonymously).

First, we assume that the tracer signal of a water mass is advected without any further dilution from the North Sea into the Arctic Ocean. Even in this simple case, a single measured ^{129}I or ^{236}U concentration (or a $^{236}U/^{238}U$ ratio) would not always give a unique solution for the transit time of a water mass because several release times are possible (due to the shape of the $^{236}U/^{238}U$ and the ^{129}I input functions, Figures 6b and 10a). The $^{129}I/^{236}U$ input function, in contrast, shows a steep and almost monotonous rise since about 1990 (the dynamic range of the input function is indicated by the dashed line in Figure 10b). Therefore, the measured $^{129}I/^{236}U$ ratio will most probably yield a simple and unique solution for the transport age of a water mass that was labeled after 1990. During the same time period the $^{236}U/^{238}U$ ratios show a decreasing trend and therefore provide additional information to further constrain the tracer ages. Based on this observation we conclude that the general and simplified concept of using the combination of $^{129}I/^{236}U$ and $^{129}I/^{236}U$ ratios for the calculation of tracer ages is valid and can be applied for the calculation of transit times of Atlantic Waters in the Arctic Ocean over the past about 25 years.

In the simplified concept discussed above, the tracer signals are not further diluted while traveling throughout the Arctic Ocean. This assumption is not entirely valid since ^{236}U (and to a minor extend also ^{129}I) is present in global fallout (Figures 8 and 9). Furthermore, significant amounts of radionuclides have been discharged into Barents and Kara Sea as a result of the civil and military use of nuclear technologies by the Former Soviet Union (FSU) [*Baskaran et al.*, 1996; *Cochran et al.*, 2000; *Cooper et al.*, 1999]. As a consequence, the $^{236}U/^{238}U$ and $^{129}I/^{236}U$ ratios of a water mass that has been labeled in the North Sea will progressively (with time) change while mixing with waters labeled by other sources. No information is available on ^{236}U or ^{129}I discharges by the nuclear facilities of the FSU and data coverage for ^{129}I in Siberian Rivers is sparse (while no data exist for ^{236}U). The few existing data on ^{129}I in Siberian Rivers, however, show that the flux of ^{129}I from Ob and Yenisei Rivers into Kara Sea between 1978 and 1991 was only 0.2–0.5% of the annual discharge flux from SF and LH [*Cochran et al.*, 2000]. We consequently assume that the additional input of ^{129}I (and probably also of ^{236}U) from Siberian Rivers can be neglected.

To simulate the mixing process with GF a simple conceptual model is used. In our example (Figure 11) the year 2012 is chosen as reference year, representing the notional sampling date of a (near) surface water mass in the Arctic Ocean. If this water mass had been labeled in the North Sea in 2011, it has a tracer age of 1 year but the initial $^{129}I/^{236}U$ and $^{236}U/^{238}U$ (given by the simulated input function, triangles in Figure 11) might have been altered due to mixing with the surrounding waters carrying the GF signal of that year. Similarly, a surface water mass labeled in 1997 (tracer age of 15 years) evolves along the 15 years "iso-age"

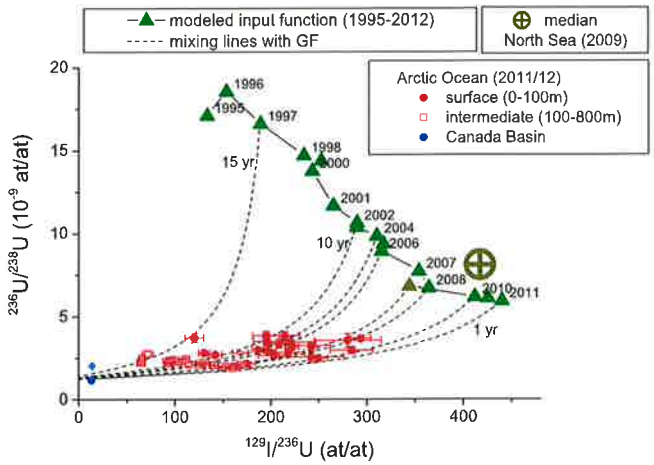

Figure 11. The dashed lines indicate the dilution of the $^{236}U/^{238}U$ and $^{129}I/^{236}U$ input function with ^{236}U and ^{129}I from global fallout (GF). The green triangles indicate the input function (without dilution). The year 2012 was used as a reference, so that waters labelled in 2011 evolve along the 1 year tracer age line while waters labeled in 1997 should plot on the 15 years tracer age line. For comparison, the measured $^{129}I/^{236}U$ and $^{236}U/^{238}U$ ratios in the North Sea (geometric mean of the 2009 data set, large cross with circle) and from the Arctic Ocean (sampled in 2011/2012) are shown. Arctic Ocean surface samples (0–100 m) are indicated by filled circles, intermediate depths (100–800 m) are represented by open squares. The surface and intermediate samples from the Canada Basin are marked in blue.

curve due to dilution with GF (dashed lines in Figure 11). In summary, when considering simple binary water mass mixing with the GF endmember all $^{129}I/^{236}U$ and $^{236}U/^{238}U$-based tracer ages lie on mixing lines with both ratios evolving from high to low values with increasing contributions from GF (dashed lines in Figure 11). Due to this dilution effect the iso-age lines tend to converge. This convergence reduces the sensitivity of the suggested method and for strongly diluted samples it might not be possible to determine a $^{129}I/^{236}U$ and $^{236}U/^{238}U$ tracer age. Nevertheless, the above calculations show that the new $^{129}I/^{236}U$ and $^{236}U/^{238}U$-based dual tracer concept generally works within certain limitations.

As a proof of concept, the model results are compared to the first available $^{129}I/^{236}U$ and $^{236}U/^{238}U$ data from the Arctic Ocean (the presentation of the whole data set is subject to a separate study, (N. Casacuberta et al., in preparation, 2015), here only the results of the surface and intermediate depth samples are presented). The conceptual tracer age model (dashed lines in Figure 11) reproduces all currently available $^{236}U/^{238}U$ and $^{129}I/^{236}U$ data from surface and intermediate depths in the Arctic Ocean (red symbols in Figure 11). Surface ratios (0–100 m, filled red dots in Figure 11) are generally higher than values found at intermediate depths (>100 – 800 m, open squares in Figure 11) indicating increasing influence of the GF source with depth. The surface and intermediate samples from the Canada Basin (blue data points in Figure 11) lie outside the dynamic range of the model because surface waters at this location are mainly of Pacific origin. The apparent tracer ages of the surface samples influenced by Atlantic Waters range between 2 years and 15 years, which is in good agreement with earlier multitracer studies [*Smith et al.*, 2011]. The fact that the iso-age lines converge with progressive dilution makes it difficult to derive precise tracer ages from samples at intermediate depths. For some of the surface samples only 1l of sea water was available for both, ^{129}I and ^{236}U analysis. Even with such small sampling volumes a precision of about 3–5 years for the final tracer age was reached. For the other surface samples (10l sampling volume) a precision of 1–3 years is generally achievable.

Although the uncertainty of the calculated tracer ages is still large, their geographic distribution (Figure 12) agrees with $^{129}I/^{137}Cs$ derived Atlantic surface water tracer ages of 3–6 years for the Kara Sea, 6–8 years for the Laptev Sea and the southern Makarov Basin, and 9–12 years for the North Pole and the Amerasian Basin [*Smith et al.*, 2011]. The distribution of the tracer ages also agrees with the fact that different branches of Atlantic waters are present in the Arctic Ocean with the youngest branch passing by Kara and Laptev Sea and older surface Waters clustering in the Amerasian Basin. Although the detailed interpretation of these apparent tracer ages is not always straightforward (and not subject to this study) our results demonstrate that the general concept of using $^{129}I/^{236}U$ and $^{236}U/^{238}U$ as a dual tracer pair is valid. The availability of the

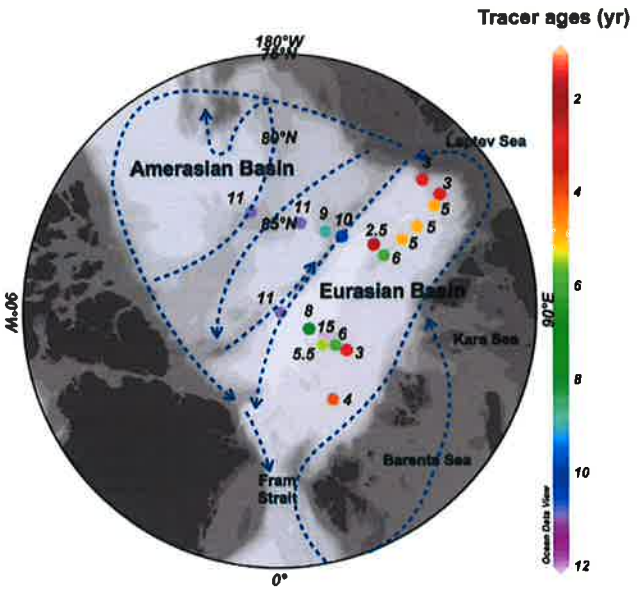

Figure 12. The geographic distribution of the calculated tracer ages (years) of surface waters (0 – 100 m) in the Arctic Ocean (2011/2012). Blue arrows represent the circulation pathways of Atlantic Waters in the Arctic Ocean.

^{236}U input function for the Northeast Atlantic Ocean provides the essential base for future studies using this tracer for determining timescales of oceanic transport or mixing processes.

4. Conclusions

The present study provided a first estimate of ^{236}U discharges into the Northeast Atlantic Ocean and presented and validated the conceptual basis for a new ^{236}U/^{238}U and ^{129}I/^{236}U-based dual tracer concept for the calculation of tracer ages.

The reconstruction of historical ^{236}U discharges into the Northeast Atlantic region was based on documented data from La Hague (France), different assumptions for the composition of U discharges from Springfields (Great Britain), and different models for the evolution of the ^{236}U/^{238}U ratio in the U discharges from Sellafield (Great Britain). According to this reconstruction a total amount of (95 $\pm$ 32) kg ^{236}U has been discharged into the Northeast Atlantic Ocean so far. This number is small compared to the global input of about 1 t ^{236}U from global fallout but it still represents the major regional source of this nuclide in the Northeast Atlantic region.

An atmospheric multibox model was coupled to a diffusive ocean surface model to estimate the spatiotemporal distribution of ^{236}U in the surface mixed layer due to global fallout only (GF-input). Further, a simple one box model was applied to simulate the evolution of the ^{236}U and ^{129}I concentrations in the North Sea using GF (^{236}U and ^{129}I) and the reconstructed (documented) releases of ^{236}U (^{129}I) as inputs. After calibration with ^{129}I, the temporal evolution of the ^{236}U/^{238}U and ^{129}I/^{236}U input functions for the Arctic Ocean were calculated.

In a second step it was shown that the combination of ^{236}U/^{238}U and ^{129}I/^{236}U in a new dual tracer concept allows the determination of transit times or tracer ages of Atlantic Waters in the Arctic Ocean over the past 25 years. To validate the new method all available data of ^{129}I/^{236}U and ^{236}U/^{238}U from the Arctic Ocean were used. The resulting tracer ages are (i) internally consistent with the modeled evolution of the tracer signal when additional dilution effects (due to GF-input) are considered and (ii) they agree well with independently derived tracer ages in the Arctic Ocean. We therefore conclude that the new, ^{236}U/^{238}U and ^{129}I/^{236}U-based dual tracer approach for the calculation of transit times of Atlantic Waters in the Arctic Ocean is valid.

The new concept is fully based on tracers that can be analyzed at ultimate sensitivity in a few liters of sea water using modern (compact) accelerator mass spectrometry methods therefore allowing its practical application in oceanographic studies where available sample volumes are always limited. Further, the dynamic range of the reconstructed $^{236}U/^{238}U$ and $^{129}I/^{236}U$ input functions allows the calculation of unequivocal tracer ages over the past about 25 years, a time range where ^{129}I or ^{236}U alone or even other classical ventilation tracers (like CFCs) would mostly fail due to their (re-)declining input function. Therefore, the new, $^{236}U/^{238}U$ and $^{129}I/^{236}U$-based dual tracer concept is well suited for the calculation of tracer ages of the rapidly circulating Atlantic Waters in the Arctic Ocean. However, the sensitivity of the new method is limited by the progressive addition (dilution) of the tracer signal with bomb derived ^{236}U (GF-input). Besides this conceptual drawback the quality of the proposed method still suffers from the poorly known input function of ^{236}U. Further studies on the historical ^{236}U content of the North Sea (e.g., using biological/carbonate archives) are needed to improve the quality of ^{236}U-based tracer ages in the Arctic Ocean. Even beyond that application, our results show that $^{236}U/^{238}U$ and $^{129}I/^{236}U$ provides a sensitive tool to study also vertical mixing processes like ventilation rates of the deep North Atlantic and Arctic Ocean.

Acknowledgments

All data used to generate figures and tables will be made available upon request to the corresponding author. Núria Casacuberta is currently funded by a SNSF Ambizione grant. The laboratory of Ion Beam Physics is partially funded by its consortium partners EAWAG, Swiss Federal Institute of Aquatic Science and Technology, EMPA, and PSI. Nicolas Houivet and Hervé Deguette (AREVA-NC Radiological Protection Department) are kindly acknowledged for providing additional data on U releases from La Hague and its isotopic composition. The authors want to thank Kirk Cochran (Stony Brook University) and an anonymous reviewer for their constructive comments that significantly improved the quality of the manuscript.

References

Alfimov, V., A. Aldahan, and G. Possnert (2004), Tracing water masses with 129I in the western Nordic Seas in early spring 2002, *Geophys. Res. Lett.*, *31*, L19305, doi:10.1029/2004GL020863.

Alfimov, V., G. Possnert, and A. Aldahan (2006), Anthropogenic iodine-129 in the Arctic Ocean and Nordic Seas: Numerical modeling and prognoses, *Mar. Pollut. Bull.*, *52*(4), 380–385.

Bailly du Bois, P., P. Guéguéniat, R. Gandon, R. Léon, and Y. Baron (1993), Percentage contribution of inputs from the Atlantic, Irish Sea, English Channel and Baltic into the North Sea during 1988: A tracer-based evaluation using artificial radionuclides, *Neth. J. Sea Res.*, *31*(1), 1–17, doi:10.1016/0077-7579(93)90012-H.

Bailly du Bois, P., F. Dumas, L. Solier, and C. Voiseux (2012), In-situ database toolbox for short-term dispersion model validation in macro-tidal seas, application for 2D-model, *Cont. Shelf Res.*, *36*, 63–82, doi:10.1016/j.csr.2012.01.011.

Baskaran, M., S. Asbill, P. Santschi, J. Brooks, M. Champ, D. Adkinson, M. R. Colmer, and V. Makeyev (1996), Pu, 137Cs and excess 210Pb in Russian Arctic sediments, *Earth Planet. Sci. Lett.*, *140*(1–4), 243–257, doi:10.1016/0012-821X(96)00040-4.

Broecker, W. S., and T. H. Peng (1982), *Tracers in the Sea*, 690 pp., Columbia Univ., N. Y.

Bullister, J. L. (2014), Atmospheric CFC-11, CFC-12, CFC-113, CCl4 and SF6 histories, Carbon Dioxide Information Analysis Center, Oak Ridge Nat. Lab., US Department of Energy, Oak Ridge, Tenn., doi:10.3334/CDIAC/otg.CFC_ATM_Hist_2014. [Available at http://cdiac.ornl.gov/ftp/oceans/CFC_ATM_Hist/CFC_ATM_Hist_2014.]

Casacuberta, N., M. Christl, J. Lachner, M. R. van der Loeff, P. Masqué, and H. A. Synal (2014), A first transect of ^{236}U in the North Atlantic Ocean, *Geochim. Cosmochim. Acta*, *133*, 34–46, doi:10.1016/j.gca.2014.02.012.

Christl, M., J. Lachner, C. Vockenhuber, O. Lechtenfeld, I. Stimac, M. R. van der Loeff, and H.-A. Synal (2012), A depth profile of uranium-236 in the Atlantic Ocean, *Geochim. Cosmochim. Acta*, *77*, 98–107, doi:10.1016/j.gca.2011.11.009.

Christl, M., J. Lachner, C. Vockenhuber, I. Goroncy, J. Herrmann, and H.-A. Synal (2013), First data of Uranium-236 in the North Sea, *Nucl. Instrum. Methods Phys. Res., Sect. B*, *294*, 530–536, doi:10.1016/j.nimb.2012.07.043.

Christl, M., et al. (2015), Status of 236U analyses at ETH Zurich and the distribution of ^{236}U and ^{129}I in the North Sea in 2009, *Nucl. Instrum. Methods Phys. Res., Sect. B*, *361*, 510–516, doi:10.1016/j.nimb.2015.01.005.

Cochran, J. K., S. B. Moran, N. S. Fisher, T. M. Beasley, and J. M. Kelley (2000), Sources and transport of anthropogenic radionuclides in the Ob River system, Siberia, *Earth Planet. Sci. Lett.*, *179*(1), 125–137, doi:10.1016/S0012-821X(00)00110-2.

Cooper, L. W., T. Beasley, K. Aagaard, J. M. Kelley, I. L. Larsen, and J. M. Grebmeier (1999), Distributions of nuclear fuel-reprocessing tracers in the Arctic Ocean: Indications of Russian river influence, *J. Mar. Res.*, *57*(5), 715–738, doi:10.1357/002224099321560546.

De Wilde, P., M. Jenness, and G. Duineveld (1992), Introduction into the ecosystem of the North Sea: Hydrography, biota, and food web relationships, *Aquat. Ecol.*, *26*(1), 7–18, doi:10.1007/bf02298024.

Eigl, R., M. Wallner, M. Srncik, P. Steier, and S. Winkler (2011), The suitability of ^{236}U as an ocean tracer, *Mineral. Mag.*, *75*(3), 802.

Elsässer, C., D. Wagenbach, I. Levin, A. Stanzick, M. Christl, A. Wallner, S. Kipfstuhl, I. K. Seierstad, H. Wershofen, and J. Dibb (2015), Simulating ice core 10Be on the glacial–interglacial timescale, *Clim. Past*, *11*(2), 115–133, doi:10.5194/cp-11-115-2015.

Fair, D. R. R., and J. N. Tweedy (1957), The discharge of radioactive liquid effluent to sea from the indscale works, Sellafield, *Windscale Rep.*, *5006*(2), 1–91.

Hamilton, E. I. (2001), Depleted uranium (DU): A holistic consideration of DU and related matters, *Sci. Total Environ.*, *281*(1–3), 5–21, doi:10.1016/S0048-9697(01)01033-6.

Hamilton, E. I., and H. E. Stevens (1985), Some observations on the geochemistry and isotopic composition of uranium in relation to the reprocessing of nuclear fuels, *J. Environ. Radioact.*, *2*(1), 23–40, doi:10.1016/0265-931X(85)90023-2.

He, P., A. Aldahan, G. Possnert, and X. L. Hou (2013), A summary of global 129I in marine waters, *Nucl. Instrum. Methods Phys. Res., Sect. B*, *294*(0), 537–541, doi:10.1016/j.nimb.2012.08.036.

Herrmann, J., P. j. Kershaw, P. B. du Bois, and P. Guegueniat (1995), The distribution of artificial radionuclides in the English Channel, southern North Sea, Skagerrak and Kattegat, 1990–1993, *J. Mar. Syst.*, *6*(5–6), 427–456, doi:10.1016/0924-7963(95)00026-L.

Hou, X., V. Hansen, A. Aldahan, G. Possnert, O. C. Lind, and G. Lujaniene (2009), A review on speciation of iodine-129 in the environmental and biological samples, *Anal. Chim. Acta*, *632*(2), 181–196, doi:10.1016/j.aca.2008.11.013.

Karcher, M. J., S. Gerland, I. H. Harms, M. Iosjpe, H. E. Heldal, P. J. Kershaw, and M. Sickel (2004), The dispersion of 99Tc in the Nordic Seas and the Arctic Ocean: A comparison of model results and observations, *J. Environ. Radioact.*, *74*(1–3), 185–198, doi:10.1016/j.jenvrad.2004.01.026.

Karcher, M., J. N. Smith, F. Kauker, R. Gerdes, and W. M. Smethie (2012), Recent changes in Arctic Ocean circulation revealed by iodine-129 observations and modeling, *J. Geophys. Res.*, *117*, C08007, doi:10.1029/2011JC007513.

Levin, I., T. Naegler, B. Kromer, M. Diehl, R. J. Francey, A. J. Gomez-Pelaez, L. P. Steele, D. Wagenbach, R. Weller, and D. E. Worthy (2010), Observations and modelling of the global distribution and long-term trend of atmospheric $^{14}CO_2$, *Tellus, Ser. B*, *62*(1), 26–46, doi: 10.1111/j.1600-0889.2009.00446.x.

Michel, R., et al. (2012), Iodine-129 and iodine-127 in European seawaters and in precipitation from Northern Germany, *Sci. Total Environ.*, *419*, 151–169, doi:10.1016/j.scitotenv.2012.01.009.

Neghabian, A.-R., Deutschland, and N. u. R. Bundesministerium für Umwelt (1991), *Verwendung von wiederaufgearbeitetem Uran und von abgereichertem Uran*, grm, Vertriebsservice Merkel, Eggenstein-Leopoldshafen.

Nies, H. (1990), The contamination of the North Sea by artificial radionuclides during the year 1987, *J. Environ. Radioact.*, *11*(1), 55–70, doi: 10.1016/0265-931X(90)90043-U.

Orre, S., J. Smith, V. Alfimov, and M. Bentsen (2010), Simulating transport of ^{129}I and idealized tracers in the northern North Atlantic Ocean, *Environ. Fluid Mech.*, *10*(1), 213–233, doi:10.1007/s10652-009-9138-3.

OSPAR (2009), *OSPAR Comission Work Areas/Radioactive Substances/Publications, Publ. 543/2011*, OSPAR Commission, London, U. K. [Available at http://www.ospar.org/.]

Peterson, K. R. (1970), An empirical model for estimating world-wide deposition from atmospheric nuclear detonations, *Health Phys.*, *18*(4), 357–368.

Povinec, P. P., P. Bailly du Bois, P. J. Kershaw, H. Nies, and P. Scotto (2003), Temporal and spatial trends in the distribution of 137Cs in surface waters of Northern European Seas—A record of 40 years of investigations, *Deep Sea Res., Part II*, *50*(17–21), 2785–2801, doi: 10.1016/S0967-0645(03)00148-6.

Raisbeck, G. M., F. Yiou, Z. Q. Zhou, and L. R. Kilius (1995), 129I from nuclear fuel reprocessing facilities at Sellafield (U.K.) and La Hague (France); potential as an oceanographie tracer, *J. Mar. Syst.*, *6*(5–6), 561–570, doi:10.1016/0924-7963(95)00024-J.

Sakaguchi, A., K. Kawai, P. Steier, F. Quinto, K. Mino, J. Tomita, M. Hoshi, N. Whitehead, and M. Yamamoto (2009), First results on ^{236}U levels in global fallout, *Sci. Total Environ.*, *407*(14), 4238–4242.

Sakaguchi, A., A. Kadokura, P. Steier, Y. Takahashi, K. Shizuma, M. Hoshi, T. Nakakuki, and M. Yamamoto (2012), Uranium-236 as a new oceanic tracer: A first depth profile in the Japan Sea and comparison with caesium-137, *Earth Planet. Sci. Lett.*, *333–334*, 165–170, doi: 10.1016/j.epsl.2012.04.004.

Scottish Environment Protection Agency (SEPA) (2010), *Radioactivity in Food and the Environment (RIFE)*, SEPA, Stirling, U. K.

Smith, J. N., K. M. Ellis, and L. R. Kilius (1998), 129I and 137Cs tracer measurements in the Arctic Ocean, *Deep Sea Res., Part I*, *45*(6), 959–984, doi:10.1016/S0967-0637(97)00107-6.

Smith, J. N., E. P. Jones, S. B. Moran, W. M. Smethie, and W. E. Kieser (2005), Iodine 129/CFC 11 transit times for Denmark Strait Overflow Water in the Labrador and Irminger Seas, *J. Geophys. Res.*, *110*, C05006, doi:10.1029/2004JC002516.

Smith, J. N., F. A. McLaughlin, W. M. Smethie, S. B. Moran, and K. Lepore (2011), Iodine-129, 137Cs, and CFC-11 tracer transit time distributions in the Arctic Ocean, *J. Geophys. Res.*, *116*, C04024, doi:10.1029/2010JC006471.

Steier, P., et al. (2008), Natural and anthropogenic ^{236}U in environmental samples, *Nucl. Instrum. Methods Phys. Res., Sect. B*, *266*(10), 2246–2250.

UNSCEAR (2000), Sources and effects of ionizing radiation ANNEX C: Exposures from man-made sources of radiation. *Rep.*, United Nations Scientific Committee on the Effects of Atomic Radiation, N. Y.

Vockenhuber, C., N. Casacuberta, M. Christl, and H.-A. Synal (2015), Accelerator Mass Spectrometry of 129I towards its lower limits, *Nucl. Instrum. Methods Phys. Res., Sect. B*, *361*, 445–449, doi:10.1016/j.nimb.2015.01.061.

Wikipedia (2015), *List of Nuclear Reactors*.

Winkler, S., P. Steier, and J. Carilli (2011), 100-year Record of $^{236}U/^{238}U$ in coral as a step towards establishing ^{236}U as oceanic tracer, *Mineral. Mag.*, *75*(3), 2167.

WISE (2014), *WISE Uranium Project*, Peter Diehl, Arnsdorf, Germany.

Wix, L. F. U., F. Morley, R. J. Garner, and J. C. Dalton (1965), A review of the liquid effluent discharges and marine monitoring programme at Windscale Works 1959–1963, report 56, U. K. At. Energy Auth., Berkshire.

Wolf, S. F., D. L. Bowers, and J. C. Cunnane (2005), Analysis of high burnup spent nuclear fuel by ICP-MS, *J. Radioanal. Nucl. Chem.*, *263*(3), 581–586, doi:10.1007/s10967-005-0627-7.

Wright, D. G., and T. F. Stocker (1992), Sensitivities of a zonally averaged global ocean circulation model, *Journal of Geophysical Research: Oceans*, *97*(C8), 12707–12730, doi:10.1029/92JC01168.